

# Flexible Microstrip Patch Antenna Design on Jeans Substrate Radiating at 2.45 GHz for WBAN Application

Saikumar Mulkalla, Avish Fakirde, and Paritosh D. Peshwe\*

*Department of Electronics and Communication Engineering, Indian Institute of Information Technology, Nagpur, Maharashtra, India*

**ABSTRACT:** This study presents a compact, low-profile, and flexible fabric antenna specifically designed for on-body Wireless Body Area Networks operating within the Industrial, Scientific, and Medical (ISM) frequency band at a central frequency of 2.45 GHz. The proposed antenna employs a jeans substrate, with a dielectric constant  $\epsilon_r = 1.67$  and loss tangent  $\tan \delta = 0.025$ , which is 0.5 mm in thickness, allowing for its flexibility. The antenna incorporates slots on the patch and a Defected Ground Structure (DGS), with a total size of  $36 \times 55 \times 0.6 \text{ mm}^3$  ( $0.29\lambda_o \times 0.45\lambda_o \times 0.005\lambda_o \text{ mm}^3$ ). To assess the antenna's flexibility, bending analysis was performed, while its performance was evaluated using a phantom model that simulates human tissue, comprising skin, fat, and bone, with respective thicknesses of 1 mm, 0.5 mm, and 4 mm. The final model of the antenna operates at a central frequency of 2.45 GHz, with an impressive bandwidth of 0.8 GHz. The proposed design maintains a high level of directivity, gain, and reflection coefficient ( $S_{11}$ ) at the desired frequency, with values of 4.7 dBi, 3.6 dBi, and  $-41 \text{ dB}$ , respectively. The Specific Absorption Rate (SAR) of the final antenna was measured on the above model and found to be  $0.114 \text{ W/Kg}$  for 1 g of tissue, which is well within the limits established by IEEE and FCC standards. Both the measured and simulated values of return loss and gain suggest that the proposed antenna is eminently suitable for body-worn applications.

## 1. INTRODUCTION

A Wireless Body Area Network (WBAN) is a wireless network that employs wearable devices to monitor and transmit various physiological signals. WBANs have garnered considerable attention in recent years owing to their potential applications in healthcare [1], sports [2], and entertainment [3]. Antenna plays a critical role in a WBAN as it is responsible for transmitting and receiving data between wearable devices and the network. However, traditional antennas are often rigid, causing discomfort when being worn for extended periods, thereby limiting their potential use in wearable devices.

Flexible antennas offer a promising solution for comfortable and continuous monitoring of physiological signals in wearable technology. They are lightweight, conform to the body's shape, and are crafted using flexible materials. These materials are finding applications in the advancement of implantable devices used in healthcare, such as endoscopy, neural recording, glucose monitoring, and intracranial pressure monitoring [4]. Their incorporation allows for improved functionality and performance in these critical healthcare areas.

Antennas are classified into wired and planar types based on their physical structure. Wired antennas, such as straight wire, loop, or dipole antennas, are low-cost but unsuitable for flexibility. Planar antennas are preferred for flexibility due to their ability to conform to surfaces, lightweight nature, low profile, and high performance. Among the available planar antennas, microstrip patch antenna stands out as the best option for flexible antenna design, owing to its low profile, lightweight

construction, ease of manufacture, and versatility across various applications, including wearables, biomedical sensors, and portable devices. The microstrip patch antenna's planar structure, miniaturization, and stable performance on the human body make it particularly popular in wearable antenna design [5].

Literature has provided different types of flexible and wearable antennas that have been studied over the years. In a study conducted by the authors of [6], a quasi-Yagi antenna resonating at 1.5835 GHz was designed. While the antenna was found to be a compact and efficient directive radiator, the substrate used was not ideal for a flexible antenna. Another study by the authors of [7] focused on designing a compact and flexible slot antenna with potential for improved gain and specific absorption rate (SAR). A low-profile triangular patch antenna with a Koch fractal design was designed in [8], offering a compact size but with a limitation of little impedance fractional bandwidth (7.75% at the resonate frequency of 2.45 GHz). A meander-line antenna was also designed in [9] for head imaging, but the overall dimensions were found to be too large for the use in compact environments. Finally, a compact planar dipole antenna having center frequency at 2.47 GHz was proposed in [10], but was limited by its large overall dimensions and minimal gain. These antenna designs have certain limitations, such as increased size, thickness, narrower bandwidth, and higher back radiation, which restrict their suitability for flexible and wearable devices.

The utilization of textile materials as substrates for antennas is becoming increasingly popular, particularly in the context of wearable medical devices. Textile antennas provide a

\* Corresponding authors: Paritosh D. Peshwe (paritoshpeshwe@gmail.com).

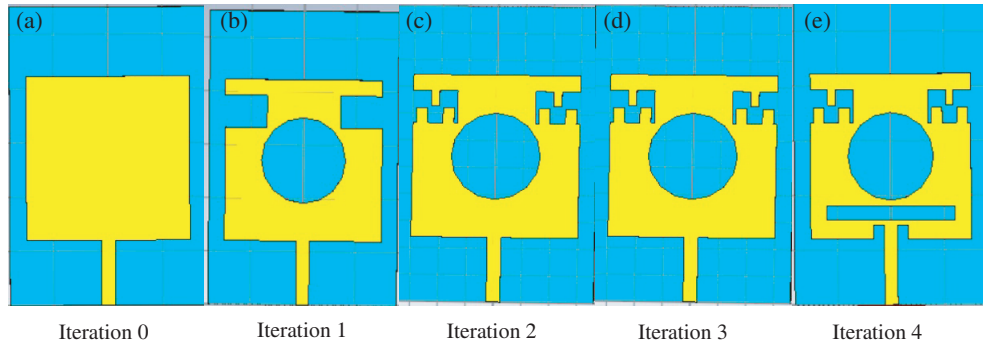


**FIGURE 1.** Evolution of patch from iteration 0 to iteration 4.

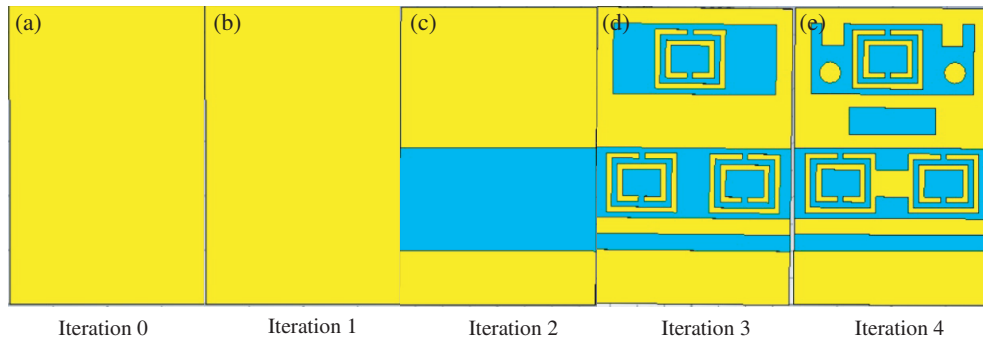


**FIGURE 2.** Evolution of ground plane from iteration 0 to iteration 4.

flexible and comfortable solution when being integrated into a patient's clothing, ensuring that monitoring data remains unaffected while offering enhanced convenience [11]. Jeans material is a suitable choice for patch antenna design due to its high flexibility, availability, high dielectric constant, and low loss tangent, which contribute to the antenna's good performance. Additionally, jeans material is low cost, easy to manufacture, and more durable than other substrates such as cotton and paper.

In [12], a patch antenna with a partial ground plane on a substrate made of jeans material was designed. However, the measurements of the antenna were quite large, and it exhibited lower gain at lower frequencies. Similarly, [13] describes an inverted F antenna on jeans substrate, but with a relatively low gain that could be improved, and [14] presents a PIFA antenna designed on a jeans substrate, but its radiation efficiency is low.

This study focuses on the design and evaluation of a flexible antenna integrated with a Defected Ground Structure (DGS), which was implemented on a Jeans substrate. The main objective was to assess the effectiveness and safety of this newly proposed antenna. Notably, this antenna boasts a thinner profile compared to previous models, and it was found to exhibit a Specific Absorption Rate (SAR) that falls well below the limits set by Federal Communications Commission (FCC) and IEEE Standards, ensuring compliance with safety regulations [15].

The structure of this paper is as follows. In Section 2, a comprehensive explanation is provided regarding the design of the antenna, along with the iterative process employed to achieve the final topology of the proposed antenna. Section 3 focuses

on the simulation and performance analysis of the finalized antenna. Finally, in Section 4, the study concludes by summarizing the key findings and drawing meaningful conclusions from the research conducted.

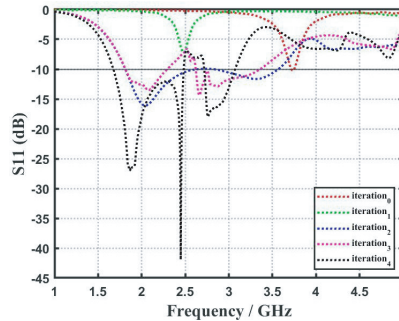
## 2. ANTENNA DESIGN

In [16], various substrate materials were discussed for antenna fabrication, and it was determined that a Jeans material (with  $\epsilon_r = 1.67$  and loss tangent = 0.025) having a thickness of 0.5 mm was used as a substrate to achieve the desired flexibility for the antenna. A  $50\Omega$  transmission line backed with a defected ground structure (DGS) was employed to excite the radiating element. To begin with, the measurements of the patch and feed were determined by applying standard equations specifically developed for microstrip patch antennas, as outlined in [17]. The ultimate configuration of the antenna represents a modified version of the regular patch antenna. Notably, the ground plane was altered, and slots were etched into it to achieve resonance at the intended frequency and attain substantial gain.

The design process began with the conventional patch antenna with a full ground in iteration 0 as shown in Figures 1(a) and 2(a). This antenna had a resonance at around 3.732 GHz and a gain of 0.377 dBi. To shift the resonance to the desired frequency, the antenna was modified in iteration 1 as shown in Figure 1(b) and 2(b), by etching a circular slot and two rectangular slots on the patch to divert the current path, thereby increasing the electrical length of the antenna and shifting the resonance to the left. At this iteration, the antenna resonated

**TABLE 1.** Optimized design parameters of proposed antenna in Figure 5(a) and 5(b).

Dimensions (unit: mm)							
$W_s = 36$	$L_s = 55$	$W_p = 30$	$L_p = 30.25$	$W_f = 2.5$	$L_f = 12$	$W1 = 8$	$L1 = 6$
$W2 = 2.5$	$L2 = 24$	$W3 = 2$	$L3 = 2.8$	$W4 = 1.5$	$L4 = 2.8$	$W5 = 2$	$L5 = 2.5$
$R = 8$	$Lg1 = 10$	$Lg2 = 3$	$Lg3 = 26$	$Lg4 = 4$	$Lg5 = 5$	$Wg1 = 4$	$Wg2 = 16$
$Wg3 = 6$	$g1 = 3$	$g2 = 13$	$g3 = 3$	$g4 = 3$	$g5 = 2$	$g6 = 10$	$g7 = 2.5$
$SL = 11$	$SW = 13$	$Rg = 2$		$h = 0.5$			$t = 0.05$

**FIGURE 3.** Variation of reflection coefficient ( $S_{11}$ ) with iterations

at 2.48 GHz, but the  $S_{11}$  value was not below  $-10$  dB, and the gain was also negative. To make the  $S_{11}$  value below  $-10$  dB, impedance matching was required, and the DGS structure could significantly improve the gain of the antenna [18]. Therefore, The antenna design underwent modifications from iteration 1 to iteration 2 as shown in Figures 1(c) and 2(c) by placing extra copper in the top rectangular slots so that the effective gap decreased, and a rectangular slot was cut down in the ground. These slots increased the capacitance of the antenna, which matched the impedance, and the DGS improved the gain. At this iteration, the antenna resonated at 2.04 GHz; the  $S_{11}$  was below  $-10$  dB; and it had a better gain than the previous iteration.

To shift the resonance to 2.45 GHz, iteration 3 introduced further modifications to enhance the antenna design previously modified in iteration 2 as shown in Figures 1(d) and 2(d) by placing split-ring resonators on the ground plane. Split-ring resonators can act as an artificial magnetic conductor (AMC) when placed on a grounded dielectric substrate. The addition of extra copper reduced the capacitance, shifting the resonance to the right while maintaining or improving the gain. In this iteration, the antenna resonated at 2.66 GHz; the  $S_{11}$  was below  $-10$  dB; and it had a gain of 3.66 dBi. The antenna was further modified in iteration 4 as shown in Figures 1(e) and 2(e) by etching a horizontal rectangular slot and two small slots beside the feed the patch. The ground plane was modified by adding copper between and adjacent to the split rings. These slots contributed to an increase in capacitance and electrical length of the antenna, resulting in the antenna resonating at the desired frequency.

In the fourth iteration, which corresponds to the proposed antenna design, resonance was achieved at a frequency of 2.45 GHz. This design exhibited a  $-10$  dB bandwidth rang-

ing from 1.68 GHz to 2.48 GHz, with an  $S_{11}$  value of  $-41$  dB specifically at the resonant frequency of 2.45 GHz. Moreover, the antenna showcased a fractional bandwidth of 38.5% and a peak gain of 3.6 dBi. The proposed antenna exhibits overall dimensions of  $36 \text{ mm} \times 55 \text{ mm} \times 0.6 \text{ mm}$  ( $0.29\lambda_o \text{ mm} \times 0.45\lambda_o \text{ mm} \times 0.005\lambda_o \text{ mm}$ ). The design evolution steps of the patch and ground plane, along with their corresponding  $S_{11}$  and gain of the antenna, are illustrated in Figures 1, 2, 3, and 4, respectively. Figures 5(a) and 5(b) exhibit the superior top and bottom views of the proposed antenna, respectively. Table 1 presents the optimized attributes of the antenna obtained after the final iteration. Figures 5(c), 5(d), and 5(e) aptly showcase the surface current density of the antenna at the 2.45 GHz frequency.

### 3. PERFORMANCE ANALYSIS OF PROPOSED ANTENNA

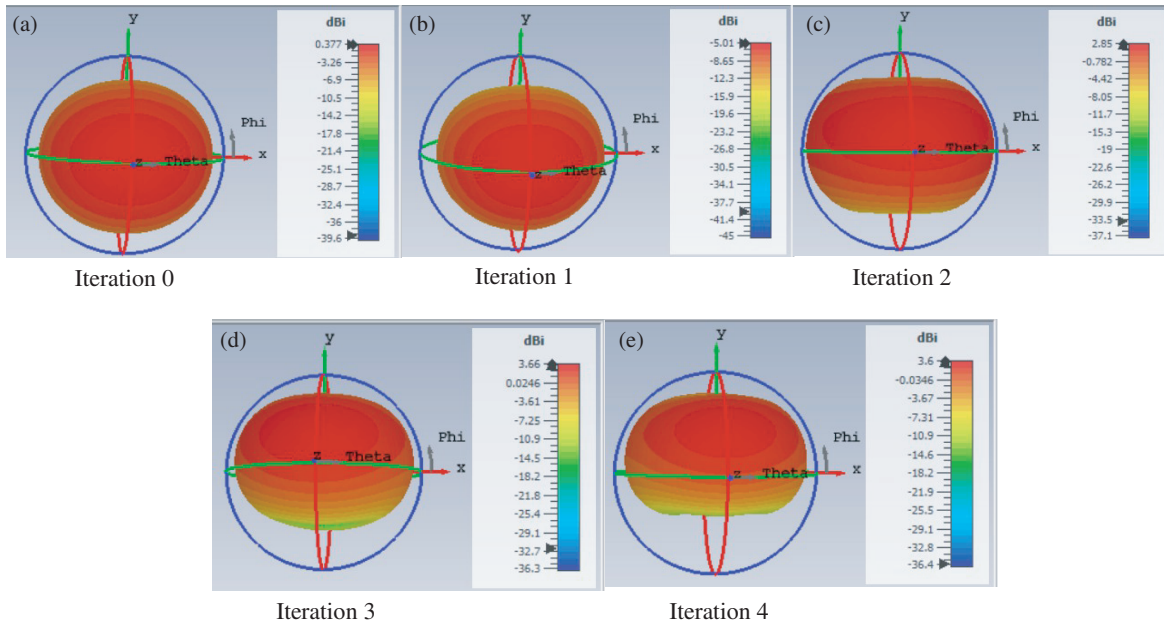
The antenna was simulated using the Computer Simulation Technology (CST) software. Figures 6(a) and 6(b) depict the fabricated antenna. The investigation of its on-body performance was conducted by establishing a three-layer human tissue phantom model measuring  $30 \text{ mm} \times 45 \text{ mm} \times 5.5 \text{ mm}$  in CST Microwave Studio, as illustrated in Figure 7. The details of the phantom model are listed in Table 2. The proposed antenna was tested on a Vector Network Analyzer, as shown in Figure 8.

#### 3.1. $S_{11}$ Parameter

Figure 9 illustrates the simulated, measured, and human tissue phantom model  $S_{11}$  values of the proposed antenna. The simulated  $S_{11}$  at 2.45 GHz is  $-41$  GHz with a  $-10$  dB impedance

**TABLE 2.** Properties of human tissue phantom model.

Tissue	Skin	Fat	Bone
Dielectric Constant ( $\epsilon$ )	36.6	10.4	16.9
Conductivity [ $\sigma$ (S/m)]	2.34	0.502	1.4
Density [ $\rho$ (kg/m <sup>3</sup> )]	1060	900	1300
Thickness (mm)	1	0.5	4

**FIGURE 4.** Variation of radiation pattern (gain) of antenna from iteration 0 to iteration 4.

bandwidth of 0.8 GHz (1.68 GHz to 2.48 GHz) and a fractional bandwidth of 38.5%.

The measured  $S_{11}$ , while slightly differing from the simulated values, still demonstrates a band of 2.4–2.5 GHz, with a value of  $-22$  dB at 2.45 GHz. The difference between these values can be attributed to fabrication and soldering errors. However, both results suggest that the proposed antenna meets the requirements of the ISM frequency band. Furthermore, the antenna was tested on a human tissue phantom model, yielding an  $S_{11}$  value of  $-17.5$  dB at 2.5 GHz with a  $-10$  dB impedance bandwidth of 1.208 GHz (1.552 GHz to 2.76 GHz) and a fractional band-width of 56%, fulfilling the necessary requirements.

Notably, the  $S_{11}$  responses of the examined antenna on the human tissue phantom model demonstrate a remarkable correspondence with the measured  $S_{11}$  values, indicating a consistent and reliable performance.

### 3.2. Gain and Radiation Efficiency

The proposed antenna exhibited a maximum gain of 3.6 dBi at 2.45 GHz, coupled with a radiation efficiency of 77.7%, as illustrated in Figure 10. The gain values derived from both practical measurements and computational simulations of the antenna showcased remarkable consistency. The radiation pat-

terns of the antenna in the  $E$ -plane ( $\phi = 0^\circ$ ) and  $H$ -plane ( $\phi = 90^\circ$ ) were portrayed in Figures 11(a) and 11(b), respectively, both in simulation and measurement.

### 3.3. Specific Absorption Rate (SAR)

It is necessary to determine the SAR prior to using any antenna in a Wireless Body Area Network (WBAN) to ensure that it complies with safety limits [19].

SAR measures the absorption of electromagnetic energy by the human body when exposed to RF-EMF. It is expressed in W/kg and calculated as  $\text{SAR} = (\sigma E^2)/\rho$ , where  $\sigma$  is the tissue conductivity (S/m),  $E$  the electric field strength (V/m), and  $\rho$  the tissue density (kg/m<sup>3</sup>).

To mitigate the potential hazards associated with harmful radiation, the International Commission on Non-Ionizing Radiation Protection (ICNIRP) has established regulatory limitations. These guidelines stipulate that the SAR should not surpass 2.0 W/kg for 10 grams of tissue. Likewise, the Federal Communications Commission (FCC) has mandated a SAR limit of 1.6 W/kg for 1 gram of tissue.

To evaluate the suitability of the proposed antenna for on-body applications, the SAR was measured on a three-layered human tissue model with a 2 mm offset between the antenna and the model, as illustrated in Figure 12. The SAR value was

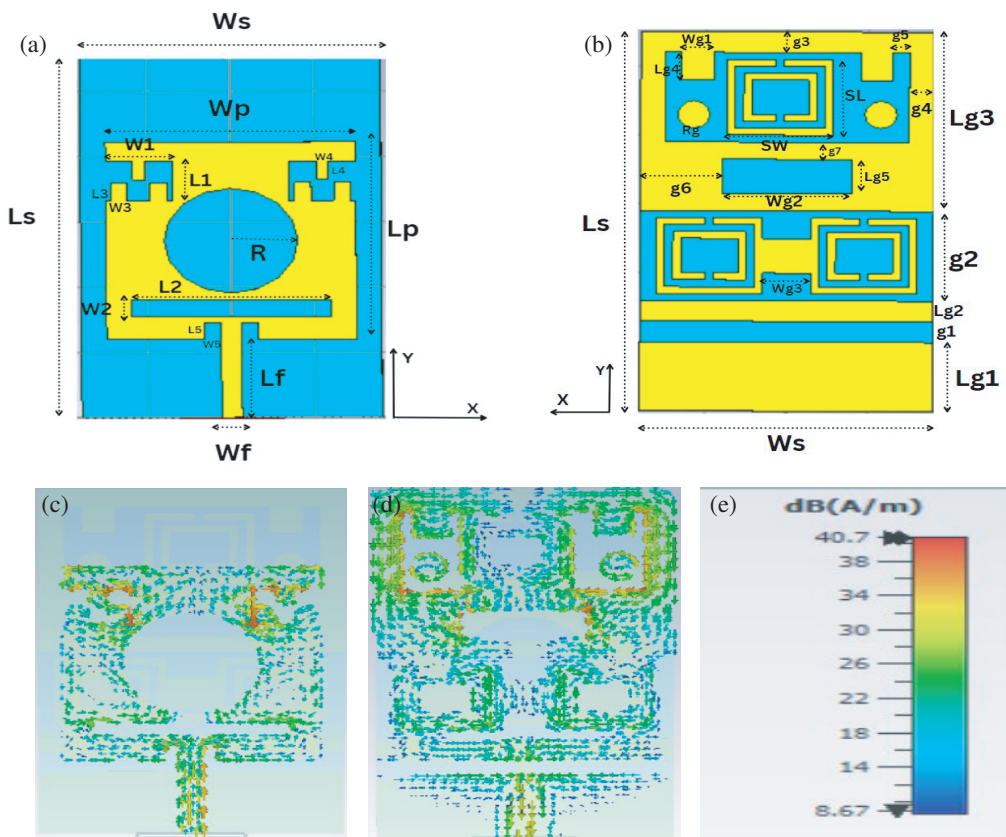


**FIGURE 5.** (a) Top view, (b) bottom view, and surface current distribution (c), (d), and (e) of the final proposed antenna at 2.45 GHz.

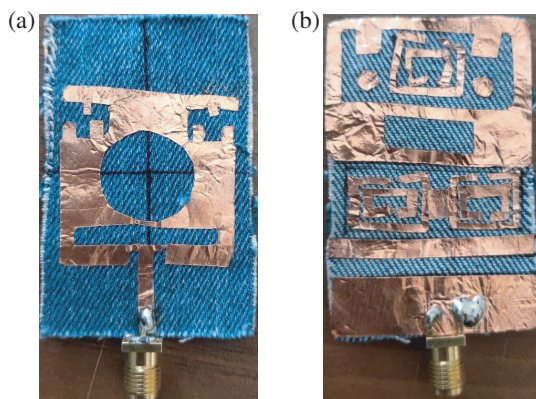


**FIGURE 6.** Fabricated proposed antenna, (a) top view and (b) bottom view.

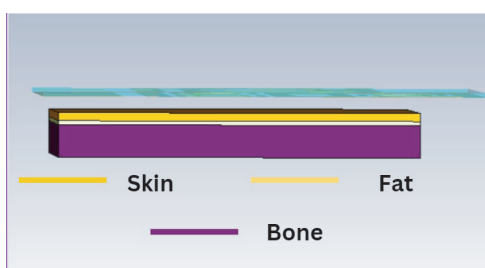


**FIGURE 7.** Human tissue phantom model.

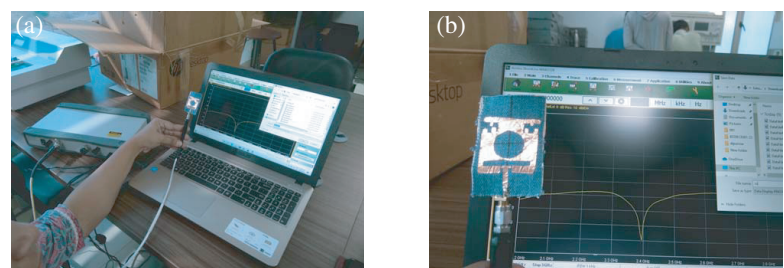


**FIGURE 8.** Testing of proposed antenna on VNA

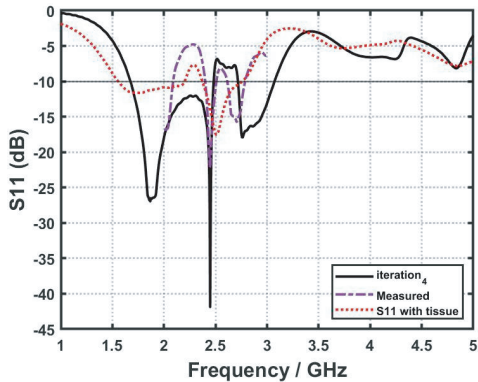


**FIGURE 9.** Simulated, measured and with human tissue reflection coefficient ( $S_{11}$ ) of proposed antenna.

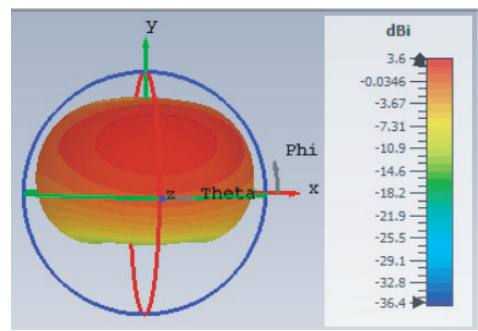


**FIGURE 10.** Gain of the proposed antenna.

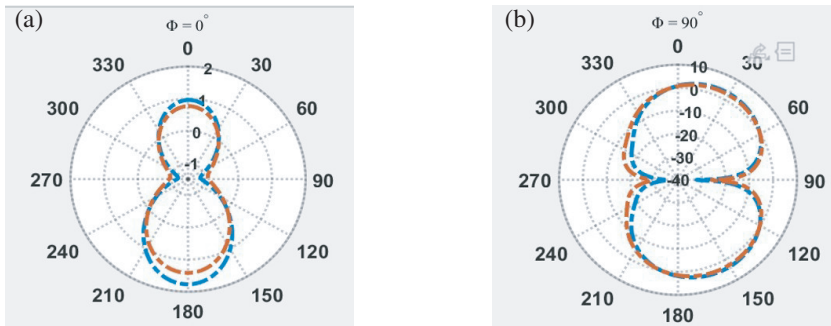


**FIGURE 11.** Radiation patterns of the designed antenna in the  $E$ -plane ( $\phi = 0^\circ$ ), and (b) in the  $H$ -plane ( $\phi = 90^\circ$ ).

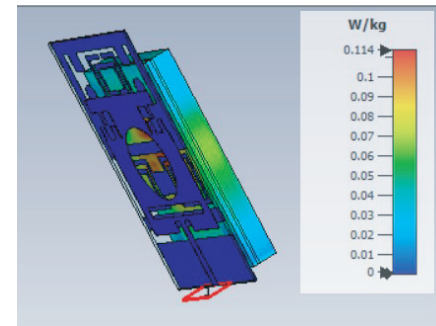


**FIGURE 12.** Measured SAR value of the proposed antenna.

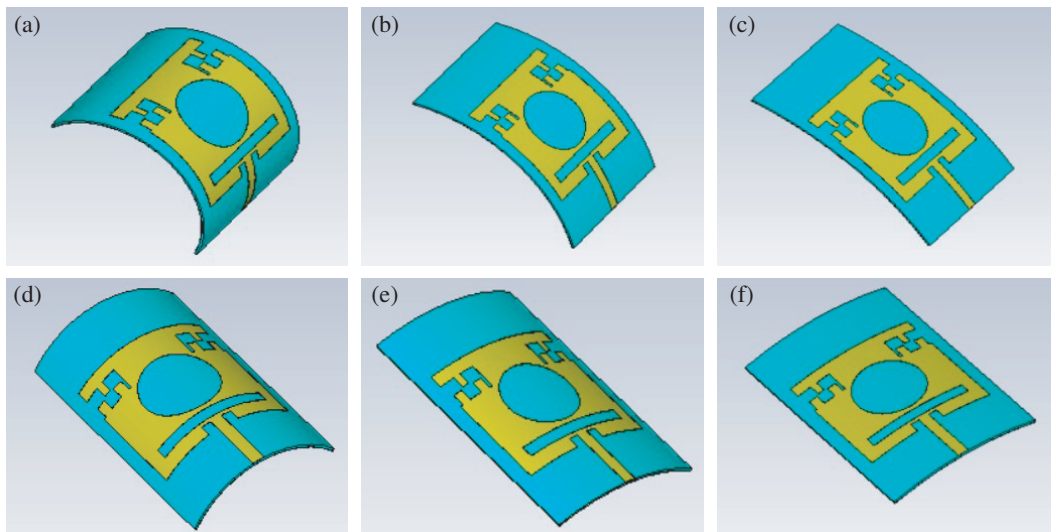


**FIGURE 13.** Structure of antenna under two bending condition with different radii, horizontal ( $x$ -axis) (a)  $R_x = 20$  mm, (b)  $R_x = 40$  mm, (c)  $R_x = 80$  mm and Vertical ( $y$ -axis) (d)  $R_y = 20$  mm, (e)  $R_y = 40$  mm, (f)  $R_x = 80$  mm.

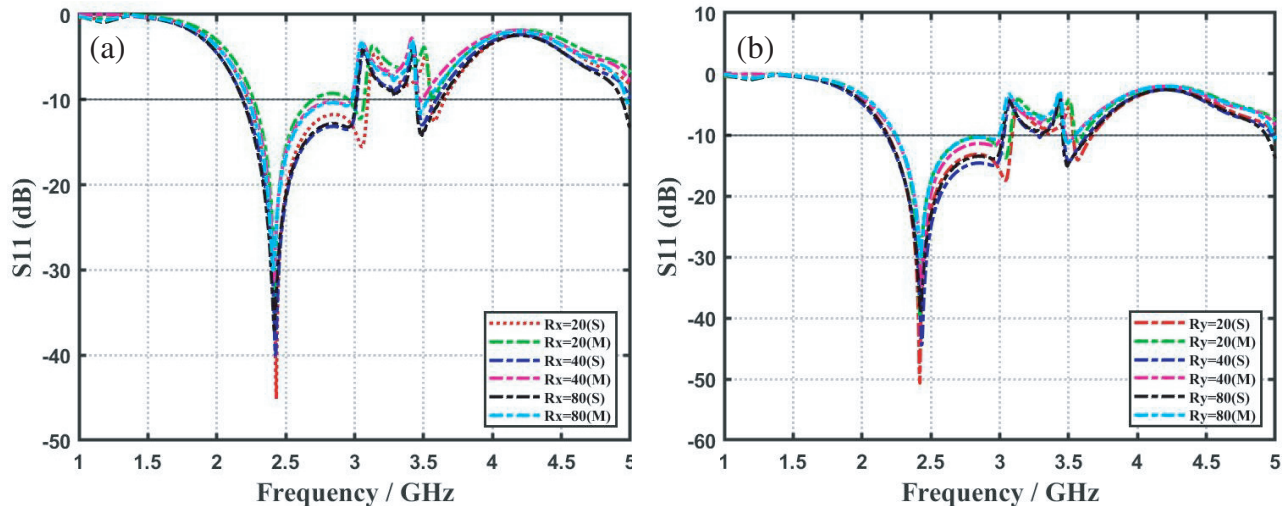


**FIGURE 14.** Measured and simulated  $S_{11}(s)$  of the proposed antenna under (a) horizontal ( $x$ -axis) and (b) vertical ( $y$ -axis) bending conditions with different curvatures.

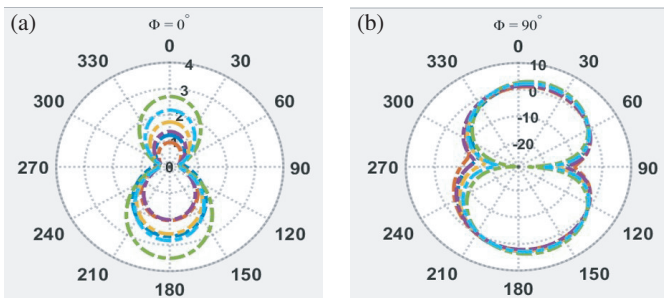


**FIGURE 15.** Radiation patterns of the designed antenna under horizontal ( $x$ -axis) bending condition in the (a)  $E$ -plane ( $\phi = 0^\circ$ ) and (b)  $H$ -plane ( $\phi = 90^\circ$ ).

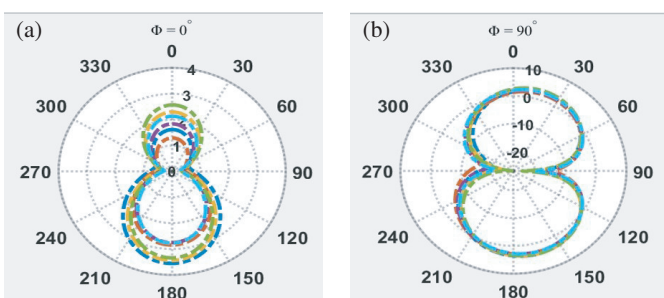


**FIGURE 16.** Radiation patterns of the designed antenna under vertical ( $y$ -axis) bending condition in the (a)  $E$ -plane ( $\phi = 0^\circ$ ) and (b)  $H$ -plane ( $\phi = 90^\circ$ ).

found to be 0.114 W/kg for 1 g of tissue, which falls well within the limits set by the FCC and IEEE standards. Based on these results, it can be concluded that the proposed antenna is well suited for on-body use.

#### 3.4. Bending Analysis

In scenarios where antennas are worn on the body, it is anticipated that they will undergo bending during use. This section presents an analysis of the antenna's performance under two bending conditions: vertical ( $y$ -axis) and horizontal ( $x$ -axis), with varying curvatures. The antenna's  $S_{11}$ , gain, and radiation pattern were studied by analysing different radii ( $R_x = 80$  mm, 40 mm, 20 mm,  $R_y = 80$  mm, 40 mm, 20 mm) along the  $x$ -axis and  $y$ -axis. The  $S_{11}$  and radiation patterns of the proposed antenna's structure under different bending conditions in the  $x$ -axis and  $y$ -axis are illustrated in Figures 13, 14, 15, and 16, respectively.

The resonance frequency for all bending scenarios exhibited minimal change, indicating that the antenna's performance is not significantly affected by bending. Moreover, the radiation patterns of the antenna remained undistorted under bending scenarios at 2.45 GHz. The antenna's gain improved under the bending scenarios. Under all bending conditions, the antenna was well matched at the targeted ISM (2.45) band. Based on this study, the proposed antenna has the potential to be utilized in applications where bending may occur.

Table 3 provides a comprehensive comparison of the antenna's performance in both unbent and bent conditions. Additionally, the study concludes that the proposed antenna is flexible.

#### 3.5. Comparison of the Proposed Antenna with Previous Work

To assess the effectiveness of the proposed antennas, a comparative analysis was carried out with existing wearable antennas,

**TABLE 3.** Comparison of antenna properties under two bending conditions with different curvatures.

Bending in $x$ -axis (Horizontal)				Bending in $y$ -axis (Vertical)			
$R_x$ (mm)	Res. freq (GHz)	$S_{11}$ (dB)	Gain (dBi)	$R_y$ (mm)	Res. freq (GHz)	$S_{11}$ (dB)	Gain (dBi)
Unbent	2.45	-41	3.6	Unbent	2.45	-41	3.6
20	2.43	-45.14	3.84	20	2.42	-50	3.94
40	2.424	-40	3.78	40	2.43	-44.5	3.89
80	2.415	-37.13	3.82	80	2.424	-39	3.9

**TABLE 4.** Comparision of proposed antenna with other wearable antennas.

Ref.	Dimensions (mm <sup>3</sup> )	Frequency (GHZ)	$S_{11}$ (dB)	Gain (dBi)	Substrate
[20]	70 × 70 × 2.26	2.36–2.40	-30	1.38	wolf felt
[21]	70 × 50 × 0.66	1.198–4.055	-26	2.9	polyester fibre
[22]	59.8 × 59.8 × 3.18	2.3–2.68	-20	2.64	pdms
[23]	85.5 × 85.5 × 5.62	1.4–2.4	-16	1.94	kelver
[24]	38.1 × 38.1 × 2	2.4–2.485	-35	2.79	felt
[25]	40 × 40 × 1.6	1.71–3.94	-30.1	1.96–2.36	fr4
[26]	72.54 × 72.54 × 1.67	2.4–2.5	-18, -23	1.92, 2.27	felt & jeans, felt & teflon
<b>Proposed Antenna</b>	36 × 55 × 0.6	1.68–2.48	-41	3.6	jeans

as detailed in Table 4. The evaluation parameters included size, substrate material and bandwidth. Based on the analysis, the proposed antenna was found to be relatively compact, exhibited satisfactory radiation performance, and complied with the prescribed SAR limits.

## 4. CONCLUSION

We have developed a compact, low-profile, and highly flexible fabric antenna suitable for the use in Wireless Body Area Networks. The miniaturization and impedance matching of the antenna have been achieved through the incorporation of rectangular and circular slots in the conventional rectangular patch. The gain of the antenna has been further improved through the use of a DGS ground plane. The antenna is resonant at 2.45 GHz with a reflection coefficient of -41 dB. Additionally, the designed antenna has a gain of 3.6 dBi, with a radiation efficiency of 77.7%. It also demonstrates exceptional performance when subjected to bending along both the  $x$  and  $y$  axes. Furthermore, the antenna complies with the strict SAR guidelines outlined by both the IEEE and FCC regulatory bodies. Overall, the proposed design exhibits superior performance and represents a highly promising solution for the use in human wearable devices.

## REFERENCES

- [1] Crosby, G. V., T. Ghosh, R. Murimi, and C. A. Chin, "Wireless body area networks for healthcare: A survey," *International Journal of Ad Hoc Sensor & Ubiquitous Computing*, Vol. 3, No. 3, 1, Jun. 1, 2012.
- [2] Fu, Y. and J. Liu, "Monitoring system for sports activities using body area networks," in *Proceedings of The 8th International Conference on Body Area Networks*, 408–413, 2013.
- [3] Sun, Y., D. A. Greaves, G. Orgs, A. F. De C. Hamilton, S. Day, and J. A. Ward, "Using wearable sensors to measure interpersonal synchrony in actors and audience members during a live theatre performance," *Proceedings of The ACM on Interactive Mobile Wearable and Ubiquitous Technologies-IMWUT*, Vol. 7, No. 1, 1–29, Mar. 2023.
- [4] Smida, A., A. Iqbal, A. J. Alazemi, M. I. Waly, R. Ghayoula, and S. Kim, "Wideband wearable antenna for biomedical telemetry applications," *IEEE Access*, Vol. 8, 15 687–15 694, 2020.
- [5] Gao, G.-P., C. Yang, B. Hu, R.-F. Zhang, and S.-F. Wang, "A wide-bandwidth wearable all-textile PIFA with dual resonance modes for 5 GHz WLAN applications," *IEEE Transactions on Antennas and Propagation*, Vol. 67, No. 6, 4206–4211, Jun. 2019.
- [6] Tang, M.-C., T. Shi, and R. W. Ziolkowski, "Flexible efficient quasi-Yagi printed uniplanar antenna," *IEEE Transactions on Antennas and Propagation*, Vol. 63, No. 12, 5343–5350, Dec. 2015.
- [7] Das, S. and D. Mitra, "A compact wideband flexible implantable slot antenna design with enhanced gain," *IEEE Transactions on Antennas and Propagation*, Vol. 66, No. 8, 4309–4314, Aug.

- 2018.
- [8] Arif, A., M. Zubair, M. Ali, M. U. Khan, and M. Q. Mehmood, "A compact, low-profile fractal antenna for wearable on-body WBAN applications," *IEEE Antennas and Wireless Propagation Letters*, Vol. 18, No. 5, 981–985, May 2019.
- [9] Alqadami, A. S. M., A. E. Stancombe, K. S. Bialkowski, and A. Abbosh, "Flexible meander-line antenna array for wearable electromagnetic head imaging," *IEEE Transactions on Antennas and Propagation*, Vol. 69, No. 7, 4206–4211, Jul. 2021.
- [10] Al-Sehemi, A. G., A. A. Al-Ghamdi, N. T. Dishovsky, N. T. Atanasov, and G. L. Atanasova, "Flexible and small wearable antenna for wireless body area network applications," *Journal of Electromagnetic Waves and Applications*, Vol. 31, No. 11–12, 1063–1082, 2017.
- [11] Li, Y. J., Z. Y. Lu, and L. S. Yang, "CPW-fed slot antenna for medical wearable applications," *IEEE Access*, Vol. 7, 42 107–42 112, 2019.
- [12] Nanda, C. K., S. Ballav, A. Chatterjee, and S. K. Parui, "A body wearable antenna based on jeans substrate with wide-band response," in *2018 5th International Conference on Signal Processing and Integrated Networks (SPIN)*, 474–477, Feb. 22–23 2018.
- [13] El Hajj, W., C. Person, and J. Wiart, "A novel investigation of a broadband integrated inverted-F antenna design; Application for wearable antenna," *IEEE Transactions on Antennas and Propagation*, Vol. 62, No. 7, 3843–3846, Jul. 2014.
- [14] Gil, I. and R. Fernandez-Garcia, "Wearable PIFA antenna implemented on jean substrate for wireless body area network," *Journal of Electromagnetic Waves and Applications*, Vol. 31, No. 11–12, 1194–1204, 2017.
- [15] Synopsis of IEEE std c95.1™-2019, "IEEE standard for safety levels with respect to human exposure to electric, magnetic, and electromagnetic fields, 0 Hz to 300 GHz," *IEEE Access*, Vol. 7, 171 346–171 356, 2019.
- [16] Noor, S. K., N. Ramli, N. Ramli, and N. L. Hanapi, "A review of the wearable textile-based antenna using different textile materials for wireless applications," *Open Journal of Science and Technology*, No. 3, 2020.
- [17] Balanis, C. A., *Antenna Theory: Analysis and Design*, John Wiley & Sons, 2015.
- [18] Ashyap, A. Y. I., S. H. Bin Dahlan, Z. Z. Abidin, M. H. Dahri, H. A. Majid, M. R. Kamarudin, S. K. Yee, M. H. Jamaluddin, A. Alomainy, and Q. H. Abbasi, "Robust and efficient integrated antenna with EBG-DGS enabled wide bandwidth for wearable medical device applications," *IEEE Access*, Vol. 8, 56 346–56 358, 2020.
- [19] Wang, M., Z. Yang, J. Wu, J. Bao, J. Liu, L. Cai, T. Dang, H. Zheng, and E. Li, "Investigation of SAR reduction using flexible antenna with metamaterial structure in wireless body area network," *IEEE Transactions on Antennas and Propagation*, Vol. 66, No. 6, 3076–3086, Jun. 2018.
- [20] Yang, H. and X. Liu, "Wearable dual-band and dual-polarized textile antenna for on- and off-body communications," *IEEE Antennas and Wireless Propagation Letters*, Vol. 19, No. 12, 2324–2328, Dec. 2020.
- [21] Lin, X., Y. Chen, Z. Gong, B.-C. Seet, L. Huang, and Y. Lu, "Ultrawideband textile antenna for wearable microwave medical imaging applications," *IEEE Transactions on Antennas and Propagation*, Vol. 68, No. 6, 4238–4249, Jun. 2020.
- [22] Simorangkir, R. B. V. B., Y. Yang, K. P. Esselle, and B. A. Zeb, "A method to realize robust flexible electronically tunable antennas using polymer-embedded conductive fabric," *IEEE Transactions on Antennas and Propagation*, Vol. 68, No. 6, 50–58, 2018.
- [23] Joshi, R., E. F. N. M. Hussin, P. J. Soh, M. F. J. Los, H. Lago, A. A. Al-Hadi, and S. K. Podilchak, "Dual-band, dual-sense textile antenna with AMC backing for localization using GPS and WBAN/WLAN," *IEEE Access*, Vol. 8, 89 468–89 478, 2020.
- [24] Li, H., S. Sun, B. Wang, and F. Wu, "Design of compact single-layer textile MIMO antenna for wearable applications," *IEEE Transactions on Antennas and Propagation*, Vol. 66, No. 6, 3136–3141, Jun. 2018.
- [25] Iqbal, A., A. Smida, A. J. Alazemi, M. I. Waly, N. K. Mallat, and S. Kim, "Wideband circularly polarized MIMO antenna for high data wearable biotelemetric devices," *IEEE Access*, Vol. 8, 17 935–17 944, 2020.
- [26] Mustafa, A. B. and T. Rajendran, "An effective design of wearable antenna with double flexible substrates and defected ground structure for healthcare monitoring system," *Journal of Medical Systems*, Vol. 43, No. 7, 186, Jul. 2019.